Inorganic Chemistry

Article

Synthesis, Structure, and Electrochemistry of Di- and Zerovalent Nickel, Palladium, and Platinum Monomers and Dimers Derived from an Enantiopure (*S,S*)-Tetra(tertiary Phosphine)

Heather J. Kitto, A. David Rae, Richard D. Webster,[‡] Anthony C. Willis, and S. Bruce Wild*

Research School of Chemistry, Australian National University, Canberra, Australian Capital Territory 0200, Australia

The ligand (*S,S*)-1,1,4,7,10,10-hexaphenyl-1,4,7,10-tetraphosphadecane, (*S,S*)-tetraphos, reacts with hexa(aqua)-nickel(II) chloride in the presence of trimethylsilyl triflate (TMSOTf) in dichloromethane to give the yellow square-planar complex [Ni{(*R,R*)-tetraphos}](OTf)$_2$, which has been crystallographically characterized as the square-pyramidal, acetonitrile adduct [Ni(NCMe){(*R,R*)-tetraphos}]OTf. Cyclic voltammograms of the nickel(II) complex in dichloromethane and acetonitrile at 20 °C showed two reduction processes at negative potentials with oxidative (E_p^{ox}) and reductive (E_p^{red}) peak separations similar to those observed for ferrocene/ferrocenium under identical conditions, suggesting two one-electron steps. The cyclic voltammetric data for the divalent nickel complex in acetonitrile at temperatures below −20 °C were interpreted according to reversible coordination of acetonitrile to the nickel(I) and nickel(0) complexes. The divalent palladium and platinum complexes [M{(*R,R*)-tetraphos}](PF$_6$)$_2$ and [M$_2${(*R,R*)-tetraphos}$_2$](OTf)$_4$ have been prepared. The reduction potentials for the complexes [M{(*R,R*)-tetraphos}](PF$_6$)$_2$ increase in the order nickel(II) < palladium(II) < platinum(II). The reaction of (*S,S*)-tetraphos with bis(cycloocta-1,5-diene)nickel(0) in benzene affords orange [Ni{(*R,R*)-tetraphos}], which slowly rearranges into the thermodynamically more stable, yellow, double-stranded helicate [Ni$_2${(*R,R*)-tetraphos}$_2$]; the crystal structures of both complexes have been determined. The reactions of (*S,S*)-tetraphos with [M(PPh$_3$)$_4$] in toluene (M = Pd) or benzene (M = Pt) furnish the double-stranded helicates [M$_2${(*R,R*)-tetraphos}$_2$]; the palladium complex crystallizes from hot benzene as the *2-benzene solvate* and was structurally characterized by X-ray crystallography. In each of the three zerovalent complexes, the coordinated (*R,R*)-tetraphos stereospecifically generates tetrahedral M(PP)$_2$ stereocenters of *M* configuration.

Introduction

Aggregation in coordination complexes is facilitated by dynamic dative bonding between the donor atoms of the ligands and the metal ions. Depending upon the bonding modes and geometric constraints of the ligands, in particular rigidity, and the preferred coordination geometries of the metal ions, frequently tetrahedral, a variety of interesting structural motifs can be generated under equilibrium conditions by the judicious choice of metal and ligand. Thus, with use of semirigid di- and oligo-2,2′-bipyridines and related ligands in conjunction with kinetically labile metal ions favoring tetrahedral coordination, the self-assembly of double-stranded helicates, metallocatenanes, rotaxanes, molecular grids, and knots has been achieved.[1] Our work in this area has concerned the use of configurationally pure tetra- and hexa-tertiary phosphines as agents for the self-assembly of double-stranded di- and trinuclear metal helicates. Thus, the C_2-tetra(tertiary phosphine) (*S,S*)-tetraphos[2] and the homologous hexa(tertiary phosphine) (*R,S,S,R*)-hexaphos,[3] in the presence of hexafluorophosphate, combine with copper(I), silver(I), and gold(I) ions to spontaneously

* To whom correspondence should be addressed. E-mail: sbw@rsc.anu.edu.au.
‡ Present address: Division of Chemistry and Biological Chemistry, Nanyang Technological University, Singapore 637616

(1) (a) Piguet, C.; Bernardinelli, G.; Hopfgartner, G. *Chem. Rev.* **1997**, *97*, 2005−2062. (b) Swiegers, G. F.; Malefetse, T. J. *Chem. Rev.* **2000**, *100*, 3483−3537. (c) Machado, V. G.; Baxter, P. N.; Lehn, J. M. *J. Braz. Chem. Soc.* **2001**, *12*, 431−462.
(2) Airey, A. L.; Swiegers, G. F.; Willis, A. C.; Wild, S. B. *Inorg. Chem.* **1997**, *36*, 1588−1597.
(3) Bowyer, P. K.; Cook, V. C.; Gharib-Naseri, N.; Gugger, P. A., Rae, A. D.; Swiegers, G. F.; Willis, A. C.; Zank, J.; Wild, S. B. *Proc. Natl. Acad. Sci. U.S.A.* **2002**, *99*, 4877−4882.

self-assemble double-stranded helicates of the type [M$_2$-{(R,R)-tetraphos}$_2$](PF$_6$)$_2$ (M = Ag, Au) and [Cu$_3${(S,R,R,S)-hexaphos}$_2$](PF$_6$)$_3$, in which the configurations of the internal phosphorus stereocenters[4] diastereoselectively generate helicates of M or P configuration.[6] Moreover, dependent upon the relationship between the configurations of the internal donor stereocenters and the twists of the chiral ten-membered rings containing the two metal ions, δ or λ, the hexafluorophosphate salts of the helicates crystallize as DNA-like double helices or protein-like parallel helices. It was also found that the meso ligand (R*,S*)-tetraphos combines with silver(I) and gold(I) ions in the presence of hexafluorophosphate to diastereoselectively self-assemble helicates in which there is head-to-head recognition of the pairs of R and S phosphorus stereocenters in the helicate ions.[8]

Apart from the isolation and structural characterization of (M)-[Pt$_2${(R,R)-tetraphos}$_2$](CF$_3$SO$_3$)$_4$·4.5H$_2$O,[9] work on the Group 10 metals, in which one strand of tetraphos is fully coordinated to one metal or two strands to two metals, has hitherto involved the use of the racemic ligand, namely, (R*,R*)-(±)-tetraphos, or the meso diastereomer (R*,S*)-tetraphos.[10] Of particular relevance to this work, is the isolation and solution molecular weight determination of a complex having the formulation [Pt$_2$(tetraphos)$_2$], although the diastereomer of the ligand used to prepare the complex was not specified.[11] Here we report our results concerning the synthesis, structural characterization, and electrochemistry of single- and double-stranded complexes of di- and zerovalent Group 10 metals derived from homochiral (S,S)-tetraphos.

Results and Discussion

Stereochemical Considerations. The stereospecific coordination of (S,S)-tetraphos to give a tetrahedral metal stereocenter of M configuration can be rationalized by

(S,S)-tetraphos

(R,S,S,R)-hexaphos
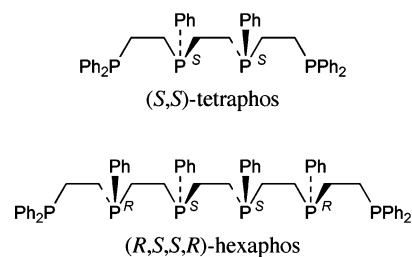
inspection of the crossed-bar diagrams shown in Figure 1a. In the figure, it can be seen that when the metal has the M configuration, the central 1,2-ethano group can effectively bridge the two inner phosphorus stereocenters of R configuration.[4] When the metal stereocenter has the P configuration, however, the estimated distance apart of the two methylene carbon atoms that would constitute the bridge is 6.41 Å. Accordingly, (S,S)-tetraphos combines with tetra(acetonitrile)copper(I) hexafluorophosphate to give (M$_{Cu}$)-[Cu{R,R)-tetraphos]PF$_6$, which has been identified by an X-ray crystal structure determination on the *1-ethanol solvate*.[2] The angle subtended by the two terminal phosphorus atoms at copper in the structure is 135.91(6)°. The strain implicit in this large angle is alleviated when the (S,S)-tetraphos combines with the larger silver(I) and gold(I) ions, where the double-stranded helicates (M$_M$,M$_M$)-[M$_2${(R,R)-tetraphos}$_2$](PF$_6$)$_2$ are formed. The ligand (S,S)-diphars, an analogue of (S,S)-tetraphos, in which the terminal phosphorus atoms have been replaced by arsenic atoms, reacts with tetra(acetonitrile)copper(I) hexafluorophosphate to give the double-stranded helicate (M$_{Cu}$,M$_{Cu}$)-[Cu$_2${(R,R)-diphars}$_2$](PF$_6$)$_2$ because of the further destabilization of the monocopper complex brought about by the relatively long copper–arsenic bonds, namely, Cu–As = 2.43 Å versus Cu–P = 2.28 Å.[12]

The helicates (M$_M$,M$_M$)-[M$_2${(R,R)-tetraphos}$_2$](PF$_6$)$_2$ (M = Ag, Au) and the closely related compounds (M$_M$,M$_M$)-[M$_2${(R,R)-diphars}$_2$](PF$_6$)$_2$ (M = Cu, Ag, Au) crystallize with idealized D$_2$ double helix or parallel structures, in which the ten-membered rings containing the two metal ions in each case have the chiral twist-boat-chair-boat (TBCB) conformation,[13] as represented by the diagrams shown in Figure 1b. In the parallel helix conformer of the helicate, the TBCB ring has a δ (clockwise) twist of 60° that is opposed to the two anticlockwise twists of ~60° of the two M(PP)$_2$ stereocenters of M configuration, which leads to a net overall helicity of ~60° for the helicate in the M direction. Each ligand strand in the parallel helicate completes ~1.5 turns of a left-handed helix down each side of the M⋯M axis. In the double-helix structure, the λ (counterclockwise) twist of ~60° of the TBCB ring augments the two twists of similar magnitude and direction for the two M(PP)$_2$ stereocenters of M configuration to give an overall twist of ~180° of each ligand strand in the M direction for the helicate. In the dinuclear metal helicates so far investigated, the more voluminous double-helix conformer of the molecules has been observed only in silver(I) complexes of (S,S)-tetraphos

(4) As a consequence of the CIP rules for specifying absolute configurations,[5] an apparent inversion of configuration occurs upon coordination of a P-chiral tertiary phosphine to an atom of atomic number greater than 12.

(5) Cahn, R. S.; Ingold, C. K.; Prelog, V. *Angew. Chem., Int. Ed. Engl.* **1966**, *5*, 385−415.

(6) Spirocyclic complexes of the type [M(AB)$_2$] may be viewed as helices, and their configuration may be denoted as P (right-handed or clockwise turns of the chelate rings when viewed *down* the principal C$_2$ axis, from either end) or M (left-handed), or they can be considered to have a chiral center, in which case they may be assigned an R (or aR) or S (aS) descriptor, respectively. The correspondence of R with M and S with P is general.[7] The P,M nomenclature is more appropriate for di- and oligonuclear metal helicates of the type considered here because the bulk helicity of a particular helicate, also designated P or M, is then a direct manifestation of the individual helicities of the chiral components along the principal axis of the helicate.

(7) Eliel, E. L.; Wilen, S. H.; Mander, L. N. *Stereochemistry of Organic Compounds*; John Wiley & Sons: New York, 1994.

(8) Blake, C. J.; Cook, V. C.; Keniry, M. A.; Kitto, H. J.; Rae, A. D.; Swiegers, G. F.; Willis, A. C.; Zank, J.; Wild, S. B. *Inorg. Chem.* **2003**, *42*, 8709−8715.

(9) Kitto, H. J.; Rae, A. D.; Willis, A. C.; Zank, J.; Wild, S. B. *Z. Naturforsch. B* **2004**, *59*, 1458−1461.

(10) The use of the relative configuration descriptors (R*,R*)-(±) and (R*,S*) for the racemic and meso diastereomers of the tetraphosphine, respectively, conforms with current *Chemical Abstracts* indexing practice and IUPAC recommendations. The enantiomers of the tetraphosphine have been given simplified descriptors.

(11) King, R. B.; Kapoor, P. N. *Inorg. Chem.* **1972**, *11*, 1524−1527.

(12) Cook, V. C.; Willis, A. C.; Zank, J.; Wild, S. B. *Inorg. Chem.* **2002**, *41*, 1897−1906.

(13) Hendrickson, J. B. *J. Am. Chem. Soc.* **1967**, *89*, 7047−7061.

(a)

(b)

(c)
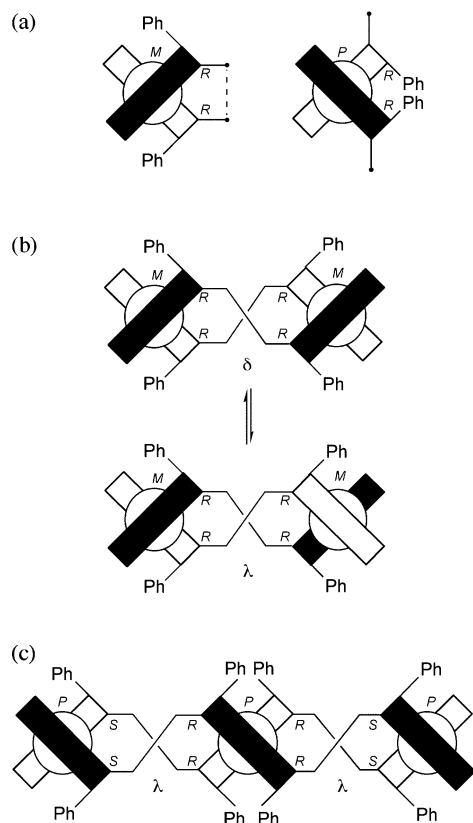
Figure 1. Chiral crossed-bar representations of the stereospecific binding of (*S*,*S*)-tetraphos to one tetrahedral metal stereocenter of *M* configuration (left) or *P* configuration (right) (a), two tetrahedral metal stereocenters of *M* configuration (b), and (*R*,*S*,*S*,*R*)-hexaphos to give three tetrahedral metal stereocenters of *P* configuration (c).[4]

and (*S*,*S*)-diphars, where it is found alongside the more compact parallel helix conformer in the unit cell of each lattice. The parallel helix is the more usual structure for univalent copper, silver, and gold complexes of the type (M_M,M_M)-[M_2{(*S*,*S*)-tetraphos}$_2$](PF$_6$)$_2$ and (M_M,M_M)-[M_2-{(*R*,*R*)-diphars}$_2$](PF$_6$)$_2$. The close relationship between the direction of the twist of the ten-membered TBCB ring containing the pairs of metal ions and the configurations of the chiral M(PP)$_2$ and M(PAs)$_2$ stereocenters in the helicates is preserved in the structure of (P_{Cu},P_{Cu},P_{Cu})-[Cu$_3${*S*,*R*,*R*,*S*}-hexaphos}$_3$](PF$_6$)$_3$·4C$_6$H$_6$, where the parallel helix conformer of the helicate is found in the crystal lattice, as represented by the diagram in Figure 1c.[3] In this structure, the two annulated ten-membered TBCB rings containing the three copper ions each have the left-handed (λ) twist; these anticlockwise twists of the TBCB rings are negated by the clockwise (*P*) twists of the three Cu(PP)$_2$ stereocenters, which results in the parallel helix conformer of the helicate, where each ligand strand completes ~2.5 turns of a *P* helix in a cation of idealized D_2 symmetry.

Synthesis of Metal Complexes. (a) Nickel. The enantiopure complex [NiCl{(*R*,*R*)-tetraphos}]Cl was prepared by the addition of a solution of [Ni(H$_2$O)$_6$]Cl$_2$ in water to a solution of (*S*,*S*)-tetraphos in dichloromethane (Scheme 1a). The addition of ethanol to the vigorously stirred mixture led to a deep red solution. Removal of the solvents from the
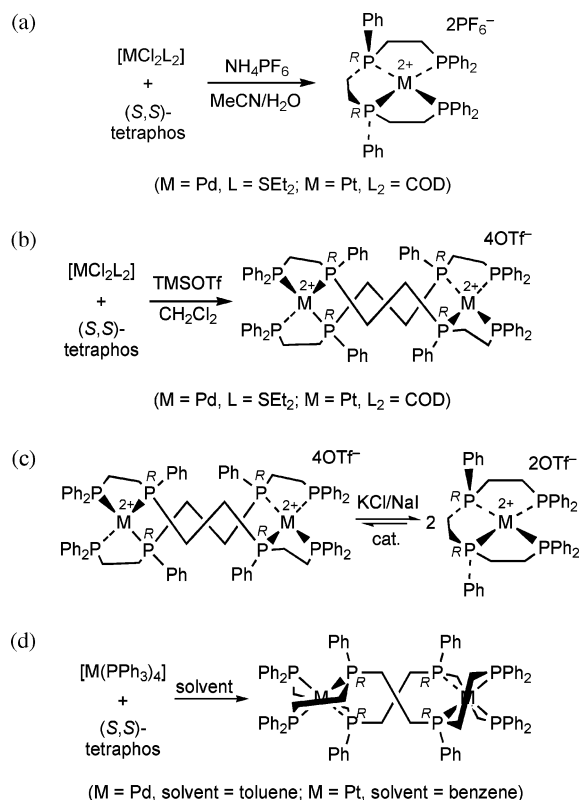
Scheme 1

(a)

(b)
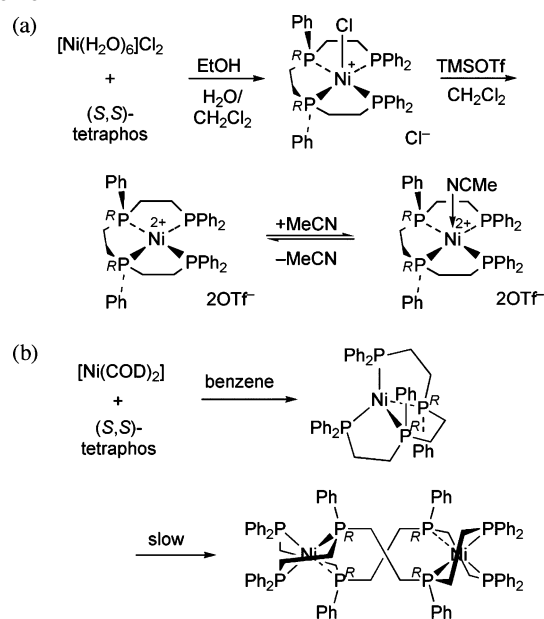
solution afforded the chloronickel(II)−tetraphos complex as a deep red-brown powder. In the ^{31}P{^{1}H} NMR spectrum in chloroform-*d*, the complex exhibits multiplets at 45.4 (PPh$_2$) and 103.5 ppm (PPh) and has [α]$^{18}_{546}$ = +16.1 (*c* 1, acetone). The addition of trimethylsilyl triflate to a solution of the *chloro* complex in dichloromethane at 0 °C resulted in an immediate color change from deep red to yellow. The removal of the solvent from the yellow solution furnished [Ni{(*R*,*R*)-tetraphos}](OTf)$_2$, which remained as a yellow solid. Redissolution of the solid in acetonitrile afforded a deep red solution of the acetonitrile adduct [Ni(NCMe)-{(*R*,*R*)-tetraphos}](OTf)$_2$ that was isolated by precipitation with diethyl ether; the dark orange-red crystals of the acetonitrile adduct lost acetonitrile upon evacuation and reverted to the original yellow, square-planar complex (mp 231−234 °C).

The neutral complex [Ni{(*R*,*R*)-tetraphos}] was prepared by the reaction of [Ni(COD)$_2$] (COD = cyclo-1,5-octadiene) with (*S*,*S*)-tetraphos in benzene (Scheme 1b). After 1 h, the orange solution was evaporated to dryness, and the orange oil that remained was dissolved in diethyl ether; the solution deposited an orange microcrystalline precipitate, which was filtered off and washed with diethyl ether to give the pure complex, having mp = 98−101 °C and [α]$^{18}_D$ = −147.9 (*c* 1, benzene). Orange solutions of the mononuclear nickel complex in diethyl ether, benzene, or toluene slowly changed (over several months) into yellow solutions of [Ni$_2${(*R*,*R*)-tetraphos}$_2$]. Orange plates of monomeric complex and yellow plates of the dimeric complex slowly crystallized above a diethyl ether solution of the monomeric complex as the solvent evaporated, both of which were shown by X-ray crystallography to contain 0.5 diethyl ether molecule of crystallization (see below).

(b) Palladium. The complex [Pd{(*R*,*R*)-tetraphos}](PF$_6$)$_2$ was prepared by the addition of [PdCl$_2$(SEt$_2$)$_2$] in acetonitrile to a suspension of (*S*,*S*)-tetraphos in the same solvent (Scheme 2a). A bright yellow solution resulted, which was

Scheme 2

(a)

(M = Pd, L = SEt₂; M = Pt, L₂ = COD)

(b)

(M = Pd, L = SEt₂; M = Pt, L₂ = COD)

(c)

(d)

(M = Pd, solvent = toluene; M = Pt, solvent = benzene)

treated with aqueous ammonium hexafluorophosphate. The solvent was removed from the solution under vacuum, and the residue was stirred in water to remove excess ammonium hexafluorophosphate and the ammonium chloride byproduct. The pale orange powder that remained was filtered off and recrystallized from acetonitrile−diethyl ether to give colorless microcrystals of the pure complex (88%), which had mp = 174 °C (dec) and $[\alpha]_D^{18} = +61.2$ (c 1.0, acetone).

The complex [Pd₂{(R,R)-tetraphos}₂](OTf)₄ was prepared by the addition of a dichloromethane solution of [PdCl₂-(SEt₂)₂] to a solution of (S,S)-tetraphos in the same solvent, as indicated in Scheme 2b. The bright yellow solution that resulted was treated with TMSOTf, whereupon there was an immediate decolorization of the solution. The solvent and trimethylsilyl chloride byproduct were removed from the reaction mixture under vacuum and the residue was dissolved in acetonitrile; dilution of the solution with diethyl ether brought about the crystallization of the dipalladium(II) complex as a colorless solid (87%), having mp = 312−315 °C and $[\alpha]_D^{18} = -311.7$ (c 1, acetone). The ³¹P{¹H} NMR spectrum of the complex was consistent with its formulation as a dimer (see below). Crystals of the complex suitable for X-ray crystallography could not be obtained. The addition of a few drops of aqueous potassium chloride (0.13 M) to a solution of [Pd₂{(R,R)-tetraphos}₂](OTf)₄ (∼50 mg) in acetone-d₆ resulted in the immediate rearrangement of the dimer into ∼40% of the monopalladium complex (Scheme 2c). After 90 days, the proportion of dimer to monomer was essentially unchanged. The addition of a trace of aqueous sodium iodide to the dipalladium complex in acetone-d₆ led to an immediate color change in the solution from colorless

to deep yellow and complete conversion into the mono-nuclear palladium complex in 8 days. The addition of an excess of a solution of either halide to an acetone-d₆ solution of the dipalladium complex resulted in immediate and complete conversion into the monopalladium complex.

The complex [Pd₂{(R,R)-tetraphos}₂] resulted from the reaction between [Pd(PPh₃)₄] and (S,S)-tetraphos in toluene (Scheme 2d). After ∼0.5 h, the bright yellow solution of the complex was filtered through Celite to remove a trace of palladium. Removal of the solvent from the filtrate left a yellow oil, which was dissolved in diethyl ether; yellow needles of the product deposited overnight from the solution. The needles were filtered off, washed with diethyl ether, and dried under vacuum to afford the dipalladium(0) complex in 85% yield, which had mp = 125−128 °C (dec) and $[\alpha]_D^{18} = +40.2$ (c 1, benzene).

(c) Platinum. The complex [Pt{(R,R)-tetraphos}](PF₆)₂ was prepared by the addition of [PtCl₂(COD)] in acetonitrile to a suspension of (S,S)-tetraphos in the same solvent (Scheme 2a). The bright yellow solution that resulted was treated with aqueous ammonium hexafluorophosphate. After removal of the solvents, the residue was stirred in water to remove excess ammonium hexafluorophosphate and the ammonium chloride byproduct. The pale yellow powder that remained was recrystallized from acetonitrile−diethyl ether to give the almost colorless product (93%), which had mp = 270−272 °C and $[\alpha]_D^{18} = -35.0$ (c 1, acetone). Crystals of the complex suitable for X-ray crystallography could not be obtained.

The diplatinum complex was prepared as the *triflate* by the addition of TMSOTf to a solution of [PtCl₂(COD)] and (S,S)-tetraphos in dichloromethane (Scheme 2b).⁹ Removal of the solvent and trimethylsilyl chloride byproduct under vacuum afforded a colorless residue that was redissolved in acetonitrile; the product, [Pt₂{(R,R)-tetraphos}₂](OTf)₂·2H₂O, was obtained from the solution by precipitation with wet diethyl ether and was isolated as a colorless solid in 91% yield (mp = 309−312 °C, $[\alpha]_D^{18} = +160$ (c 1.0, acetone)). The addition of a trace of aqueous potassium chloride to a solution of the diplatinum(II) complex in acetone-d₆ led to its gradual rearrangement into the monoplatinum(II) complex (∼95% conversion after 90 days); the conversion of dimer into monomer also occurred when aqueous sodium iodide was added, but the rate was much slower (∼40% conversion after 90 days) (Scheme 2c). The addition of an excess of aqueous chloride or iodide solution to an acetone-d₆ solution of the platinum dimer led to the immediate, complete formation of the platinum monomer.

The complex [Pt₂{(R,R)-tetraphos}₂] was prepared by the reaction of [Pt(PPh₃)₄] with (S,S)-tetraphos in benzene (Scheme 2d). After 0.5 h, the bright yellow solution was evaporated to dryness, and the yellow oil that remained was dissolved in diethyl ether; a fine yellow powder separated almost immediately. The powder was filtered off and washed with diethyl ether; the pure complex formed feathery, yellow needles (53%) having mp = 162−166 °C and $[\alpha]_D^{18} =$

Table 1. Crystallographic Data and Experimental Details for the X-ray Crystal Structure Analyses

	[Ni(NCMe)-{(R,R)-tetraphos}](OTf)$_2$	(M_{Ni})-[Ni{(R,R)-tetraphos}]·0.5Et$_2$O	(M_{Ni},M_{Ni})-[Ni$_2${(R,R)-tetraphos}$_2$]·0.5Et$_2$O	(M_{Pd},M_{Pd})-[Pd$_2${(R,R)-tetraphos}$_2$]·2C$_6$H$_6$
molecular formula	C$_{46}$H$_{45}$F$_6$NNiP$_4$S$_2$	C$_{44}$H$_{47}$NiO$_{0.5}$P$_4$	C$_{86}$H$_{89}$Ni$_2$O$_{0.5}$P$_8$	C$_{96}$H$_{96}$P$_8$Pd$_2$
fw	1068.59	766.46	1495.86	1710.33
cryst color, habit	orange, plate	orange, plate	yellow, plate	yellow, plate
crystal size (mm)	0.22 × 0.16 × 0.06	0.30 × 0.15 × 0.12	0.26 × 0.21 × 0.15	0.21 × 0.18 × 0.04
space group	$P2_12_12_1$	$P2_1$	$P2_1$	$P\bar{1}$
cryst syst	orthorhombic	monoclinic	monoclinic	triclinic
a (Å)	13.2784(1)	14.6487(2)	14.7451(2)	14.8875(8)
b (Å)	19.3240(2)	14.4641(2)	9.9707(1)	16.5889(9)
c (Å)	37.3338(4)	19.0842(2)	25.8889(2)	19.0688(11)
α (deg)				105.936(2)
β (deg)		90.1252(9)	90.3454(5)	100.285(4)
γ (deg)				90.298(3)
V (Å^3)	9579.55(16)	4043.56(9)	3806.09(7)	4448.3(4)
Z	8	4	2	2
d_{calcd} (g cm^{-3})	1.482	1.259	1.305	1.277
μ (cm^{-1})	6.98	6.69	7.08	5.92
instrument	Nonius KappaCCD	Nonius KappaCCD	Nonius KappaCCD	Nonius KappaCCD
radiation	Mo Kα	Mo Kα	Mo Kα	Mo Kα
no. unique reflns	16 875	18 351	17 368	28 412
no. reflns obsd	11 403 ($I > 3\sigma(I)$)	13 018 ($I > 3\sigma(I)$)	13 745 ($I > 3\sigma(I)$)	15 951 ($I > 3\sigma(I)$)
2θ range (deg)	6−55	6−55	6−55	6−50
scan technique	φ and ω	φ and ω	φ and ω	φ and ω
temp (K)	200	200	200	200
structural refinement	CRYSTALS[32] maXus[33]	CRYSTALS[32] maXus[33]	CRYSTALS[32] maXus[33]	RAELS2000[34]
R1^a	0.0404	0.0261	0.0255	0.080
wR2^a	0.0463	0.0250	0.0259	0.104

^{a} R1 = [$\Sigma||F_0| - |F_C||]/\Sigma|F_0|$; wR2 = $\{[\Sigma w(F_0^2 - F_C^2)^2]/[\Sigma w(F_0^2)^2]\}^{1/2}$.

−117.6 (*c* 1, benzene). The needles were not suitable for X-ray crystallography.

Crystal Structures. (a) Nickel. Dark orange plates of [Ni-(NCMe){(R,R)-tetraphos}](OTf)$_2$ crystallized from an acetonitrile solution of [Ni{(R,R)-tetraphos}](OTf)$_2$ upon the addition of diethyl ether. Crystals of the nickel(0) complexes were obtained from a diethyl ether solution: orange and yellow crystals of the complexes slowly crystallized on the walls of the flask, above the solution. X-ray crystal structure analyses identified the orange crystals as (M_{Ni})-[Ni{(R,R)-tetraphos}]·0.5Et$_2$O and the yellow crystals as (M_{Ni},M_{Ni})-[Ni$_2${(R,R)-tetraphos}]·0.5Et$_2$O. Crystallographic data and associated experimental details for the complexes are given in Table 1. The crystal structures of the racemates (±)-[NiCl-{(R^*,R^*)-tetraphos}]PF$_6$[14] and (±)-[Ni{(R^*,R^*)-tetraphos}]-(ClO$_4$)$_2$[15] have been determined previously.

The crystallographic asymmetric unit of [Ni(NCMe)-{(R,R)-tetraphos}$_2$](OTf)$_2$ consists of two distinct cations of the complex and four triflate ions (one of which is disordered). The structure of one of the two cations of the complex is shown in Figure 2; the nickel(II) ion has square-pyramidal coordination geometry, with the acetonitrile molecule occupying an apical site. The Ni−N distance in the cation is 2.018(5) Å in one independent molecule and 2.089(4) Å in the other molecule; the nickel atom in the former molecule sits 0.354 Å above the least-squares P$_4$ plane, in the direction of the acetonitrile ligand. The phosphorus atoms P1 and P3 in the cation deviate above the least-squares plane by 0.352

and 0.274 Å. As is the case with all crystallographically characterized, monomeric nickel(II)−tetraphos complexes, the distances between the nickel ion and the inner-phosphorus atoms (Ni−PPh) are shorter than those to the outer-phosphorus atoms (Ni−PPh$_2$). The central five-membered ring in the cation shown (containing P2 and P3) has a symmetric skew conformation; a counterclockwise direction of rotation is required to bring the axis passing through the two phosphorus atoms into coincidence with the non-orthogonal skew-line passing through the two carbon atoms, which leads to the assignment of λ to the conformation of the ring. The two outer five-membered chelate rings in the cation adopt enantiomorphic asymmetric envelope conformations.[16]

The crystallographic asymmetric unit of [Ni{(R,R)-tetraphos}]·0.5Et$_2$O contains two crystallographically distinct molecules in the unit cell. The structure of one of the molecules is shown in Figure 3. The coordination geometry around the nickel is tetrahedral and is similar to that of the copper in (M_{Cu})-[Cu{(R,R)-tetraphos}]PF$_6$·EtOH.[2] The *R* configurations of the inner-phosphorus stereocenters in both complexes generate metal stereocenters of *M* configuration. The three five-membered chelate rings in the complex have the symmetric skew conformation, with the twist in each case being in the counterclockwise, or λ, direction.

The crystallographic asymmetric unit of (M_{Ni},M_{Ni})-[Ni$_2$-{(R,R)-tetraphos}$_2$]·0.5Et$_2$O contains one molecule of the complex and the disordered solvent of crystallization. The coordination geometry around each nickel atom in the

(14) Airey, A. L.; Hockless, D. C. R.; Swiegers, G. F.; Wild, S. B. *Z. Kristallogr.* **1996**, *211*, 939−941.

(15) Airey, A. L.; Hockless, D. C. R.; Swiegers, G. F.; Wild, S. B. *Z. Krystallogr.* **1996**, *211*, 937−938.

(16) Hawkins, C. J. *Absolute Configurations of Metal Complexes*; Wiley-Interscience: New York, 1971; Chapter 2.
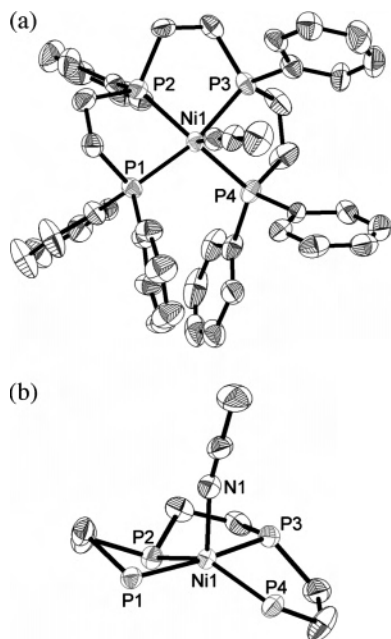
Figure 2. Molecular structure of one of the two independent molecules of [Ni(NCMe){(*R,R*)-tetraphos}]²⁺ showing 50% probability ellipsoids (a) and view showing the distorted square-pyramidal geometry of the nickel-(II) atom (b); hydrogen atoms have been omitted for clarity. Selected bond lengths (Å) and angles (deg): Ni1−P1 = 2.2236(14), Ni1−P2 = 2.1878-(14), Ni1−P3 = 2.1945(14), Ni1−P4 = 2.2515(14), Ni1−N1 = 2.018(5), P1−Ni1−P2 = 82.51(5), P1−Ni1−P3 = 167.67(6), P1−Ni1−P4 = 106.11-(5), P2−Ni1−P3 = 85.31(5), P2−Ni1−P4 = 143.60(6), P3−Ni1−P4 = 84.91(5), P1−Ni1−N1 = 89.42(13), P2−Ni1−N1 = 111.73(13), P3−Ni1−N1 = 93.35(13), P4−Ni1−N1 = 103.79(13).
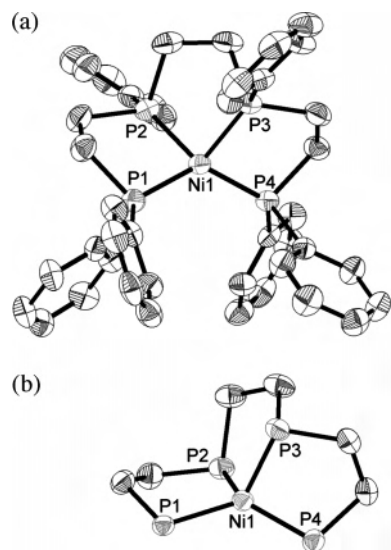
Figure 3. Molecular structure of one of the two independent molecules of (*M*$_{Ni}$,*M*$_{Ni}$)-[Ni{(*R,R*)-tetraphos}] showing 50% probability ellipsoids (a) and view showing the distorted tetrahedral geometry at nickel (b); hydrogen atoms and solvent molecules have been omitted for clarity. Selected bond lengths (Å) and angles (deg): Ni1−P1 = 2.1440(7), Ni1−P2 = 2.1254(7), Ni1−P3 = 2.1257(7), Ni1−P4 = 2.1419(6), P1−Ni1−P2 = 89.21(3), P1−Ni1−P3 = 127.73(3), P1−Ni1−P4 = 128.22(3), P2−Ni1−P3 = 92.68-(3), P2−Ni1−P4 = 127.84(3), P3−Ni1−P4 = 89.66(3).

complex is tetrahedral (Figure 4). The overall structure of the complex is similar to that of the analogous silver(I) and gold(I) complexes, where the two ligand strands wrap around each other on either side of the metal−metal axis, as shown in Figure 4b. The two nickel stereocenters in the molecule
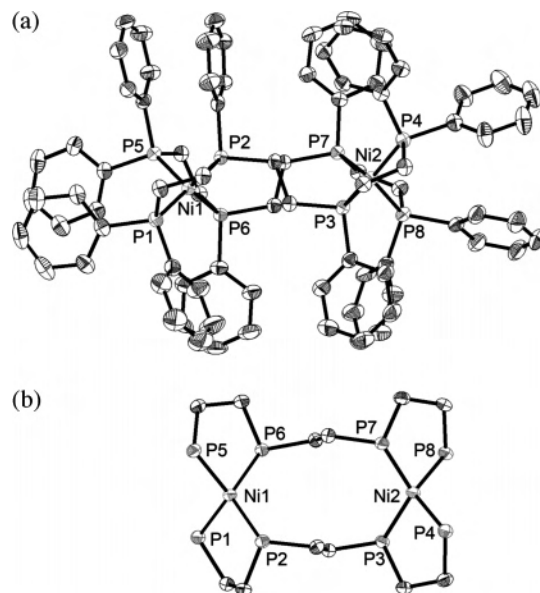
Figure 4. Molecular structure of (*M*$_{Ni}$,*M*$_{Ni}$)-[Ni₂{(*R,R*)-tetraphos}₂] showing 50% probability ellipsoids (a) and view showing the parallel arrangement of the tetraphosphine ligand strands along each side of the Ni···Ni axis (b); hydrogen atoms and solvent molecules have been omitted for clarity. Selected bond lengths (Å) and angles (deg): Ni1−P1 = 2.1659(6), Ni1−P2 = 2.1623(6), Ni1−P5 = 2.1529(6), Ni1−P6 = 2.1667(6), Ni2−P3 = 2.1689(6), Ni2−P4 = 2.1665(6), Ni2−P7 = 2.1586(6), Ni2−P8 = 2.1511-(6), Ni1···Ni2 = 6.205(1), P1−Ni1−P2 = 90.30(2), P1−Ni1−P5 = 115.47-(2), P1−Ni1−P6 = 125.78(2), P2−Ni1−P5 = 116.87(2), P2−Ni1−P6 = 119.47(2), P5−Ni1−P6 = 91.44(2), P3−Ni1−P4 = 91.52(2), P3−Ni2−P7 = 121.83(2), P3−Ni2−P8 = 117.43(2), P4−Ni2−P7 = 118.39(2), P4−Ni2−P8 = 119.27(2), P7−Ni2−P8 = 91.16(2).

have *M* configurations, which are generated by the four inner-phosphorus stereocenters of *R* configuration. The inner Ni−P(Ph) and the outer Ni−P(Ph₂) distances in the complex are similar. The Ni···Ni distance in the complex is 6.205(1) Å; the corresponding distances in the analogous silver and gold complexes are 6.072(4) and 6.244(2) Å, respectively.[2] The three five-membered rings in the dinuclear nickel complex associated with the atoms P1/P2, P3/P4, and P7/P8 have the *δ* conformation, but the five-membered ring containing P5/P6 has the *λ* conformation, which reduces the symmetry of the cation in the solid state to *C₁*. The ten-membered ring containing the two nickel atoms adopts the *δ*-TBCB conformation, which, in conjunction with the two negative twists arising from the two M(PP)₂ stereocenters of *M* configuration, generates an overall *M* twist for the parallel helix conformer of the helicate.

The differences in the P−Ni−P angles in (*M*$_{Ni}$)-[Ni{(*R,R*)-tetraphos}], (*M*$_{Ni}$,*M*$_{Ni}$)-[Ni₂{(*R,R*)-tetraphos}₂], and [Ni(dppe)₂][17] reflect the strain imposed on the tetrahedral structure by the central 1,2-ethano spacer group of the tetraphosphine ligand. The P−Ni−P angles in the three complexes (following the labeling scheme shown in Figure 5) are listed in Table 2. All of the angles in the three complexes that involve five-membered chelate rings are close to 90° because of the constraints within these rings. It is also evident in the mononuclear metal complex that the five-membered chelate ring containing the central ethylene spacer adds considerable

(17) Hartung, H.; Baumeister, U.; Walther, B.; Maschmeier, M. *Z. Anorg. Allg. Chem.* **1989**, *578*, 177−184.
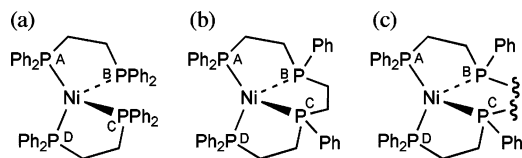
Figure 5. Atom labeling for [Ni(dppe)$_2$] (a), [Ni{(*R,R*)-tetraphos}] (b), and [Ni$_2${(*R,R*)-tetraphos}$_2$] (c).

Table 2. Core Angles (deg) in [Ni(dppe)$_2$] (a), (M_{Ni})-[Ni{(*R,R*)-tetraphos}] (b), and (M_{Ni},M_{Ni})-Ni$_2${(*R,R*)-tetraphos}$_2$] (c)

	a	b	c
P$_A$−Ni−P$_B$	90.8(1)	89.12(3)	90.30(2)
P$_A$−Ni−P$_C$	120.2(1)	127.73(3)	125.78(2)
P$_A$−Ni−P$_D$	113.8(1)	128.22(3)	115.47(2)
P$_B$−Ni−P$_C$	129.3(1)	92.68(3)	119.47(2)
P$_B$−Ni−P$_D$	114.4(1)	127.84(3)	116.87(2)
P$_C$−Ni−P$_D$	90.1(1)	89.66(3)	91.44(2)

strain to the structure; the P$_A$−Ni−P$_D$ angle in the monomer, 128.22(3)°, is much greater than the corresponding angles in the dinickel complex, 115.47(2)°, and the dppe complex, 113.8(1)°. With the exception of the large P$_B$−Ni−P$_C$ angle, the angles in [Ni(dppe)$_2$] and the dimer are similar, but they differ greatly from those in the mononuclear nickel–tetraphos complex because of the constraint placed on this molecule by the small angle P$_B$−Ni−P$_C$.

(b) Palladium. The complex (M_{Pd},M_{Pd})-[Pd$_2${(*R,R*)-tetraphos}$_2$]·2C$_6$H$_6$ crystallizes as yellow plates from benzene–diethyl ether. The crystallographic asymmetric unit of the complex contains two similar molecules and four benzene molecules of crystallization. The $Z = 2$, space group $P1$ crystal structure has four twin components in the ratio 0.540: 0.158(2):0.286(2):0.016(2), resulting from a pseudo-$P2_12_12$ interface between layers perpendicular to the c^* direction. By refining the contributions to intensities of the minor twin components as a function of spot separation in reciprocal space, we obtained a satisfactory refinement. One of the molecules is shown in Figure 6; the two palladium(0) atoms have distorted tetrahedral coordination geometries, and the overall structure of the molecule is similar to that of the corresponding dinickel(0) complex. The metal stereocenters in the palladium(0) complex have M configurations imposed by the R configurations of the inner-phosphorus stereocenters. The average M−P distances in (M_{Pd},M_{Pd})-[Pd$_2${(*R,R*)-tetraphos}$_2$] (2.338 Å) are longer than those in the nickel(0) complex (2.162 Å). The P−M−P angles in the two complexes are comparable, with the exceptions of P2−M−P5, P3−M−P7, and P3−M−P8, which are 7−11° larger in the palladium(0) complex. The Pd···Pd interatomic distance is 6.300(8) Å. Four five-membered chelate rings are present in the molecule; the rings associated with P1/P2 and P3/P4 have δ conformations, and those associated with P5/P6 and P7/P8 have λ conformations. The central ten-membered ring containing the two palladium atoms has the δ-TBCB conformation, and the two ligand strands in the molecule complete ~1.5 turns down each side of the metal−metal axis. The negative twists associated with the two Pd(PP)$_2$ stereocenters of M configuration overcome the positive twist of the TBCB ring to generate an overall parallel helicate of M
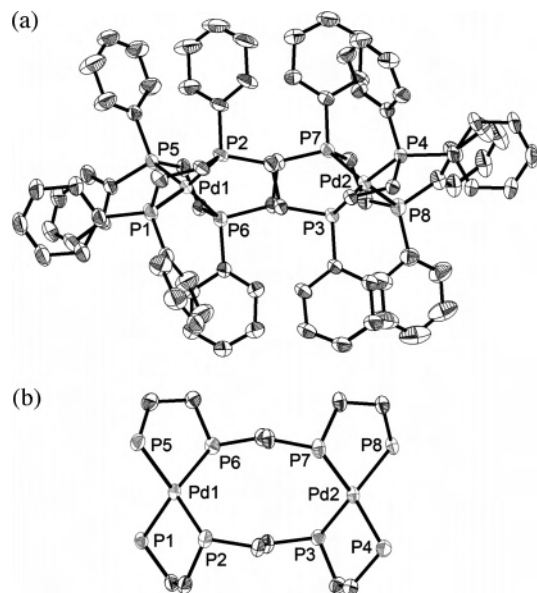
Figure 6. Molecular structure of one of two independent molecules of (M_{Pd},M_{Pd})-[Pd$_2${(*R,R*)-tetraphos}$_2$] showing 50% probability ellipsoids (a) and view showing the parallel arrangement of the tetraphosphine ligand strands down either side of the metal−metal axis (b); hydrogen atoms and solvent molecules have been omitted for clarity. Selected bond lengths (Å) and angles (deg): Pd1−P1 = 2.336(6), Pd1−P2 = 2.330(5), Pd1−P5 = 2.335(5), Pd1−P6 = 2.308(6), Pd2−P3 = 2.331(6), Pd2−P4 = 2.362(6), Pd2−P7 = 2.345(5), Pd2−P8 = 2.357(6), Pd1···Pd2 = 6.300(8), P1−Pd1−P2 = 86.6(2), P1−Pd1−P5 = 116.6(2), P1−Pd1−P6 = 128.2(2), P2−Pd1−P5 = 127.7(2), P2−Pd1−P6 = 116.8(2), P5−Pd1−P6 = 86.1(2), P3−Pd2−P4 = 86.9(2), P3−Pd2−P7 = 116.5(2), P3−Pd2−P8 = 128.4-(2), P4−Pd2−P8 = 117.4(2), P7−Pd2−P8 = 86.5(2).

configuration. The crystal structure of (±)-[Pd{(*R*,R**)-tetraphos}]Cl$_2$ has been reported previously.[18]

(c) Platinum. The crystal structure of [Pt$_2${(*R,R*)-tetraphos}$_2$]-(CF$_3$SO$_3$)$_4$·4.5H$_2$O has been reported elsewhere.[9] The cation of the salt consists of a double-stranded diplatinum(II) helicate that completes an approximately one-eighth turn of a double helix in the M direction, as measured by the angle between the two Pt(PP)$_2$ square planes. The ten-membered ring containing the two platinum atoms has a distorted twist-boat-chair-boat conformation of λ helicity, which is responsible for the M twist of the helicate. The crystal structures of (±)-[Pt{*R*,R**)-tetraphos}](BPh$_4$)$_2$,[19] [Pt{(*R*,S**)-tetraphos}]-(BPh$_4$)$_2$,[20] and (±)-[PtH{(*R*,R**)-tetraphos}]BPh$_4$[21] have been previously reported.

NMR Spectra. (a) Mononuclear Metal Complexes. The ^{31}P{^{1}H} NMR spectrum of [Ni{(*R,R*)-tetraphos}](OTf)$_2$ in acetone-d_6 corresponds to an AA′BB′ spin system because of the magnetic inequivalence of the four phosphorus nuclei. The spectrum is shown in Figure 7a and contains second-order multiplets in the vicinity of 45.5 ppm for the outer-phosphorus nuclei (PPh$_2$) and 110.3 ppm for the inner-phosphorus nuclei (PPh). These signals arise from the two overlapping and mutually coupled resonances for P$_A$ and P$_{A'}$ (45 ppm) and P$_B$ and P$_{B'}$ (110 ppm). The resonances in the

(18) Oberhauser, W.; Bachmann, C.; Brügeller, P. *Polyhedron* **1995**, *14*, 787−792.
(19) Brügeller, P.; Hübner, T. *Acta Crystallogr. C* **1990**, *46*, 388−391.
(20) Brügeller, P.; Nah, H.; Messerschmidt, A. *Acta Crystallogr. C* **1992**, *48*, 817−821.
(21) Brügeller, P. *Acta Crystallogr. C* **1992**, *48*, 445−449.
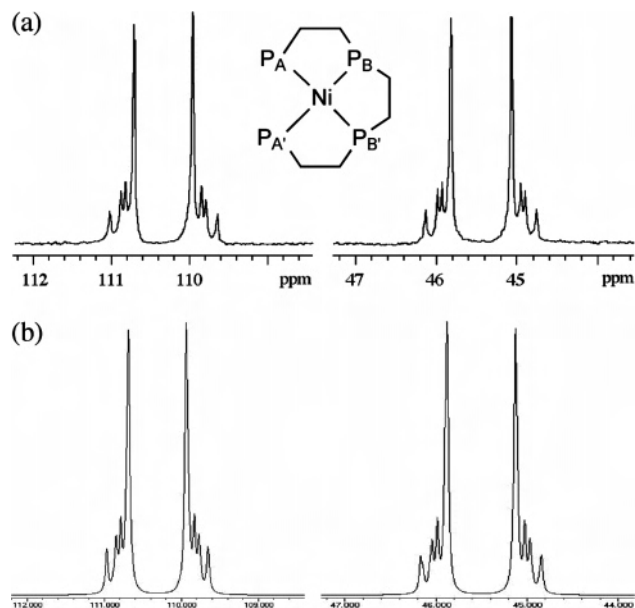
Figure 7. $^{31}P\{^1H\}$ NMR spectrum of [Ni{(R,R)-tetraphos}](OTf)$_2$ in acetone-d_6 (a) and simulated spectrum (b).

spectrum of the complex cannot be resolved by implying that the differences in chemical shifts for P$_A$ and P$_{A'}$ and P$_B$ and P$_{B'}$ are small, even within the context of second-order behavior ($\Delta A < 5J_{AA'}$). Given this constraint and the capacity for resonances within a second-order regime to exhibit different line-widths [the signs and magnitudes typically observed for P$-$P coupling constants within square-planar complexes are the following: $J_{cis} = -10$ to -50 Hz, $J_{trans} = 100-500$ Hz, and $^3J_{PP} = 20-40$ Hz (bond-mediated interactions)][22] and that $^2J_{cis}$ and $^3J_{PP}$ are rarely resolved individually, a simulation of the observed spectrum was carried out with use of the program gNMR, version 4.1.0.[23] One viable solution for the observed spectrum is shown in Figure 7b and corresponds to an AA′BB′ spin system with the following couplings: $^2J_{AA'} = -33$ Hz, $^2J_{AB'} = 177$ Hz, $^{2+3}J_{AB} = -27$ Hz, $^{2+3}J_{A'B'} = -28$ Hz, $^2J_{A'B} = 180$ Hz, and $^{2+3}J_{BB'} = 20$ Hz. The $^{31}P\{^1H\}$ NMR spectrum of the racemate (±)-[Ni{(R*,R*)-tetraphos}](BPh$_4$)$_2$ is reported to be solvent dependent.[24] For the complex [Ni{(R,R)-tetraphos}](OTf)$_2$, an upfield shift was observed for the resonances for the phosphorus nuclei in acetonitrile-d_3 compared to the values in acetone-d_6 and nitromethane-d_3, together with a slight broadening of the peaks; the latter phenomenon can be attributed to exchange of the coordinated acetonitrile with the solvent. The complex [Pd{(R,R)-tetraphos}](PF$_6$)$_2$ has a $^{31}P\{^1H\}$ NMR spectrum in acetone-d_6 similar to that of the corresponding nickel(II) complex, with the multiplets for the AA′BB′ spin system being centered at 42.2 (PPh$_2$) and 108.9 ppm (PPh). The complex [Pt{(R,R)-tetraphos}](PF$_6$)$_2$ also

gives rise to the typical AA′BB′ $^{31}P\{^1H\}$ NMR spectrum in acetone-d_6 with resonances for the cation being centered at 42.0 (PPh$_2$) and 95.7 ppm (PPh), along with $^{31}P-^{195}Pt$ coupling, namely, $^1J_{PtP} = 2133$ (PPh) and 2413 Hz (PPh$_2$).

(b) Dinuclear Metal(II) Complexes. The $^{31}P\{^1H\}$ NMR spectrum in acetone-d_6 of [Pd$_2${(R,R)-tetraphos}$_2$](OTf)$_4$ gives rise to two broad peaks at 51.6 and 56.0 ppm for the rapidly equilibrating mixture of double-helix and parallel-helix conformers. The assignment of the peaks in the spectrum to the inner- and outer-phosphorus nuclei was made by comparison with spectrum of [Pd(dppe)$_2$]Cl$_2$. The singlet peak in the $^{31}P\{^1H\}$ NMR spectrum of [Pd(dppe)$_2$]Cl$_2$ in chloroform-d occurs at 56.7 ppm;[25] on this basis, the peak at 56.0 ppm in the dipalladium(II) complex was assigned to the outer-phosphorus nuclei (PPh$_2$).

The $^{31}P\{^1H\}$ NMR spectrum of [Pt$_2${(R,R)-tetraphos}$_2$]-(OTf)$_4$ in acetone-d_6 contains two broad resonances at 42.2 (PPh) and 47.8 ppm (PPh$_2$), together with associated platinum satellites. The resonance at 47.8 ppm has been assigned to the outer-phosphorus nuclei in the complex on the basis of the similarity of the shift to that for the PPh$_2$ group in [Pt-(dppe)$_2$]Cl$_2$, namely, 47.0 ppm in benzene-d_6.[26] In the diplatinum complex, $^1J_{PtP} = 2236$ Hz (PPh) and 2405 Hz (PPh$_2$). The difference in the values of the coupling constants for the inner and outer phosphorus nuclei in the complex is similar to the difference in the couplings observed for the corresponding phosphorus nuclei in [Pt{(R,R)-tetraphos}]-(PF$_6$)$_2$.

(c) Mono- and Dinuclear Metal(0) Complexes. The $^{31}P-\{^1H\}$ NMR spectrum of [Ni{(R,R)-tetraphos] in benzene-d_6 contains apparent triplets centered at 49.5 (PPh$_2$) and 69.1 ppm (PPh). In an ideal tetrahedral system, the inner- and outer-phosphorus nuclei will each give a doublet in the spectrum. The apparent triplets in the spectrum are overlapping doublets that arise because of a lowering of symmetry of the molecule brought about by the restrictions of the ligand. The $^{31}P\{^1H\}$ NMR spectrum in benzene-d_6 of a solution of the complex after 2 months contained broad peaks at 45.4 and 48.6 ppm for [Ni$_2${(R,R)-tetraphos}$_2$]. After a further month, the NMR spectrum of the solution showed only the resonances for the dimer.

The 500 MHz $^{31}P\{^1H\}$ NMR spectrum of [Pd$_2${(R,R)-tetraphos}$_2$] at 25 °C in benzene-d_6 contains a single peak at 33.7 ppm. The 300 MHz $^{31}P\{^1H\}$ NMR spectrum in toluene-d_8 also contained a singlet, but at −40 °C, the resonance broadens and emerges as a broad doublet for the inner- and outer-phosphorus nuclei of the D_2 molecule.

The complex [Pt$_2${(R,R)-tetraphos}$_2$] exhibits multiplets at 29.2 and 38.4 ppm for the equilibrating mixture of conformers in the $^{31}P\{^1H\}$ NMR spectrum in benzene-d_6, which are superimposed on broad resonances. Both multiplets in the spectrum consist of two doublets, each being flanked by platinum satellites. The appearance of two doublets for the two types of phosphorus nuclei in the complex indicates

(22) (a) Quin, L. D., Verkade, J. G., Eds. *Phosphorus-31 NMR Spectral Properties in Compound Characterization and Structural Analysis*; VCH: New York, 1994. (b) Pregosin, P. S.; Kunz, R. W. *Phosphorus-31 and Carbon-13 NMR of Transition Metal Phosphine Complexes*; Springer-Verlag: Berlin, 1979.
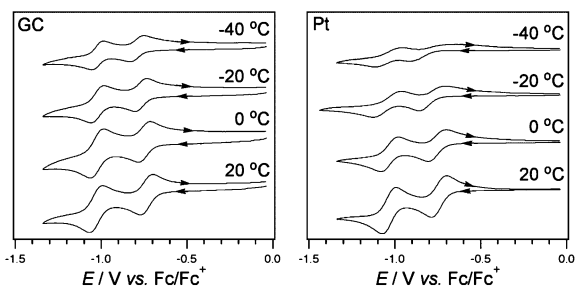(23) Budzelaar, P. H. M. *gNMR*, version 4.1.0; Cherwell Scientific Publishing: Oxford, U.K., 1995−1997.
(24) Bachmann, C.; Oberhauser, W.; Brügeller, P. *Polyhedron* **1996**, *15*, 2223−2230.

(25) Jarrett, P. S.; Ni Dhubhghaill, O. M.; Sadler, P. J. *J. Chem. Soc., Dalton Trans.* **1993**, 1863−1870.
(26) Davies, J. A.; Staples, R. J. *Polyhedron* **1991**, *10*, 899−908.

Figure 8. Cyclic voltammograms at 20 °C of a 0.5 mM solution of [Ni-{(R,R)-tetraphos}](OTf)$_2$ in dichloromethane containing 0.25 M [(n-Bu)$_4$N]-PF$_6$ at a scan rate of 100 mV s^{-1} using a GC electrode (left) and Pt electrode (right).

Figure 9. Cyclic voltammograms at 20 °C of a 0.5 mM solution of [Ni-{(R,R)-tetraphos}](OTf)$_2$ in acetonitrile containing 0.25 M [(n-Bu)$_4$N]PF$_6$ at a scan rate of 100 mV s^{-1} using a GC electrode (left) or Pt electrode (right).

Table 3. Cyclic Voltammetric Data^a for 0.5 mM Solutions of [Ni{(R,R)-tetraphos}](OTf)$_2$ in Dichloromethane and Acetonitrile Recorded at a Scan Rate of 0.1 V s^{-1} at a 1 mm Diameter Planar GC Electrode at 20 °C with 0.25 M [(n-Bu)$_4$N]PF$_6$ as the Supporting Electrolyte

solvent	E_p^{red} (V)^b	E_p^{ox} (V)^c	$E_{1/2}^r$ (V)^d	ΔE (mV)^e
CH$_2$Cl$_2$	−0.769	−0.699	−0.73	70
	−1.065	−0.990	−1.03	75
CH$_3$CN	−0.890	−0.814	−0.85	76
	−1.040	−0.960	−1.00	80

^{a} Potentials are relative to the F$_C$/F$_C^+$ redox couple. ^{b} E_p^{red} = reductive peak potential. ^{c} E_p^{ox} = oxidative peak potential. ^{d} $E_{1/2}^r = (E_p^{red} + E_p^{ox})/2$. ^{e} $\Delta E = |E_p^{ox} - E_p^{red}|$.

a distorted tetrahedral arrangement of each ligand around the metal atoms, which gives rise to four different phosphorus environments. Assignments of peaks in the ^{31}P{^{1}H} NMR spectrum of dimer in benzene-d_6 were made by comparison with those for [Pt(dppe)$_2$], which has a peak at 30.2 ppm in benzene-d_6;[27] the signal at 29.2 ppm in the dimer was accordingly assigned to the outer-phosphorus (PPh$_2$) nuclei.

Electrochemistry. The in situ UV−vis spectra of [Ni-{(R,R)-tetraphos}](OTf)$_2$ were recorded during the sequential reduction of nickel(II) to nickel(I) and nickel(0) in dichloromethane (see Supporting Information). The UV−vis spectra for the complex indicated that the electrochemical reactions were completely reversible; the starting material was regenerated by application of an oxidizing potential to the reduced solutions, and the reduced species were stable at −20 °C in this solvent.

The electrochemical properties of the nickel(II), palladium-(II), and platinum(II) complexes of (S,S)-tetraphos were investigated by cyclic voltammetry (CV). The cyclic voltammograms obtained for a dichloromethane solution containing [Ni{(R,R)-tetraphos}](OTf)$_2$ showed reduction processes at −0.73 and −1.03 V vs Fc/Fc$^+$ (Fc = ferrocene) at 20 °C. The reversible half-wave reduction potentials ($E_{1/2}^r$), which approximate the formal potentials (E^0), were calculated from the CV data under conditions where the ratio of the reductive (i_p^{red}) to oxidative (i_p^{ox}) peak currents were equal to unity, with use of the relationship $E_{1/2}^r = (E_p^{red} + E_p^{ox})/2$, where E_p^{ox} and E_p^{red} are the anodic and cathodic peak potentials, respectively (Figure 8 and Table 3). The anodic to cathodic peak-to-peak separations (ΔE_{pp}) for the reduction processes were similar to those observed for ferrocene under identical
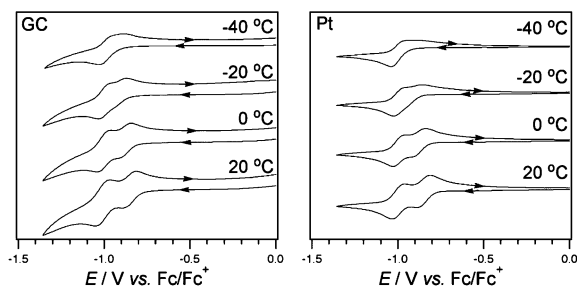
(27) Clark, H. C.; Kapoor, P. N.; McMahon, I. J. *J. Organomet. Chem.* **1984**, *265*, 107−115.

conditions, which suggests two one-electron reduction processes for the divalent metal complexes. It was therefore assumed that the first process was associated with the reduction of nickel(II) to nickel(I), and the second process was the result of the reduction of nickel(I) to nickel(0) (eqs 1 and 2).
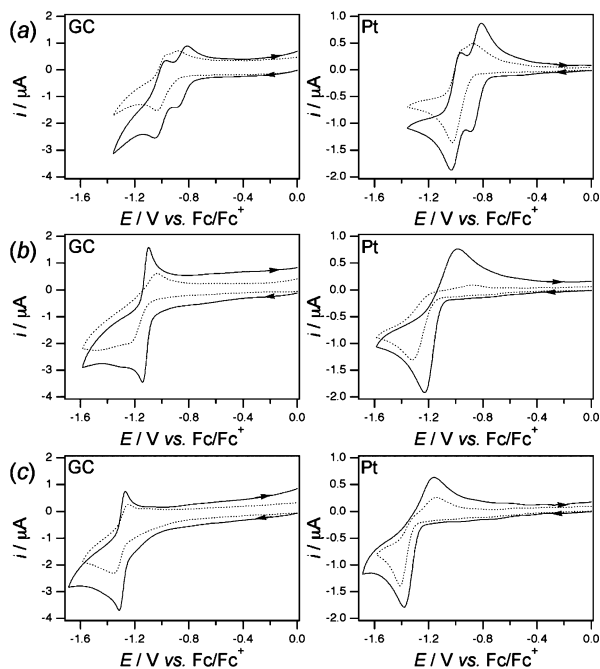
$$[\text{Ni}\{(R,R)\text{-tetraphos}\}]^{2+} + 1e^- \rightleftharpoons [\text{Ni}\{(R,R)\text{-tetraphos}\}]^+ \quad (1)$$

$$[\text{Ni}\{(R,R)\text{-tetraphos}\}]^+ + 1e^- \rightleftharpoons [\text{Ni}\{(R,R)\text{-tetraphos}\}] \quad (2)$$
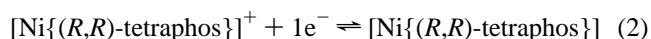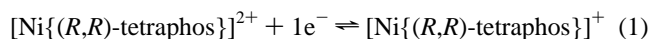
As the temperature of the solution containing [Ni{(R,R)-tetraphos}](OTf)$_2$ was lowered from 20 to −40 °C, the i_p^{red} (and i_p^{ox}) values for the complexes obtained on a glassy carbon electrode (GC) decreased because of diminishing diffusion coefficients. Below −20 °C, the i_p^{red} values observed on a platinum electrode (Pt) were lower than could be accounted for by decreasing diffusion coefficient values alone; however, the ΔE_{pp} values were larger than could reasonably be explained by increased solution resistance. Instead, it appears that the voltammetric data obtained on Pt in dichloromethane were affected by a slow rate of heterogeneous electron transfer that was most pronounced at low temperatures.

The cyclic voltammograms of [Ni{(R,R)-tetraphos}](OTf)$_2$ in acetonitrile (Figure 9) were similar to those in dichloromethane at 20 °C, but the first process was shifted by approximately −0.1 V (Table 3). As the temperature was lowered, the i_p^{red} value for the first process decreased, whereas the i_p^{red} value for the second process remained almost constant; at −40 °C, only the second process could be detected on the forward scan. Since it is expected that the peak current will decrease as the temperature is lowered because of the decreasing diffusion coefficients (as seen in dichloromethane), the apparently constant i_p^{red} value observed for the second process in acetonitrile as the temperature was lowered is most likely caused by the transfer of an increasing number of electrons (that is, the process at −1 V vs Fc/Fc$^+$ at −40 °C is associated with a two-electron transfer).
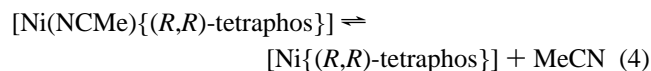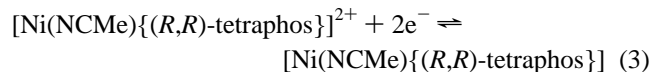
The CV data obtained in acetonitrile can most easily be accounted for by a mechanism that involves the reversible coordination of a solvent molecule to the nickel. At higher temperatures, there is a rapid equilibrium between the acetonitrile adduct [Ni(NCMe){(R,R)-tetraphos}]$^{2+}$ and its parent [Ni{(R,R)-tetraphos}]$^{2+}$, so that cyclic voltammograms detect the parent nickel(II) complex being reduced

Figure 10. Cyclic voltammograms recorded in acetonitrile containing 0.25 M [(n-Bu)₄N]PF₆ at a scan rate of 100 mV s−1 at (−−−) 20 °C and (·······) −30 °C for 0.5 mM solutions of [Ni{(R,R)-tetraphos}](OTf)₂ (a), [Pd{(R,R)-tetraphos}](PF₆)₂ (b), and [Pt{(R,R)-tetraphos}](PF₆)₂ (c) using a GC electrode (left) or Pt electrode (right).

sequentially to the corresponding nickel(I) and nickel(0) complexes (eqs 1 and 2). As the temperature of the solution is lowered to −40 °C, the position of the equilibrium changes so that only the five-coordinate complex is detected, and the CV represents the two-electron reduction of nickel(II)−MeCN to nickel(0)−MeCN (eq 3). At −40 °C, the acetonitrile−nickel(0) complex quickly dissociates into the parent nickel(0) complex and acetonitrile (eq 4, Figure 9). Thus, when the CV scan direction was reversed at −40 °C, oxidative current was observed because of the reoxidation of nickel(0) to nickel(I) and nickel(II) (the reverse of eqs 1 and 2). It was concluded from the results that the 100 mV shift in potential of the first oxidation process in acetonitrile was the result of the equilibrium that exists between the acetonitrile-free and acetonitrile−nickel(II) complexes.

$$[Ni(NCMe)\{(R,R)\text{-tetraphos}\}]^{2+} + 2e^- \rightleftharpoons$$
$$[Ni(NCMe)\{(R,R)\text{-tetraphos}\}] \quad (3)$$

$$[Ni(NCMe)\{(R,R)\text{-tetraphos}\}] \rightleftharpoons$$
$$[Ni\{(R,R)\text{-tetraphos}\}] + MeCN \quad (4)$$

Cyclic voltammograms of 0.5 mM solutions of [Pd{(R,R)-tetraphos}](PF₆)₂ and [Pt{(R,R)-tetraphos}](PF₆)₂ in acetonitrile at −30 and 20 °C are shown in Figure 10, along with cyclic voltammograms of [Ni{(R,R)-tetraphos}](OTf)₂ that were obtained under identical conditions. In general, it appears that the potential of reduction varies in the order of [Ni{(R,R)-tetraphos}]²⁺ < [Pd{(R,R)-tetraphos}]²⁺ < [Pt{(R,R)-tetraphos}]²⁺, although there are difficulties in assigning the true reduction potentials for the palladium and platinum complexes because of the complex shapes of the cyclic voltammograms. Electrochemical data for these com-

plexes were restricted to measurements in acetonitrile because of the poor solubilities of [M{(R,R)-tetraphos}(PF₆)₂ (M = Pd, Pt) in dichloromethane. The principal difference between the CV data for the three complexes is that the nickel complex displays two reduction processes in acetonitrile (at higher temperatures), whereas the palladium and platinum complexes show only one response, albeit with a complex shape. The peak currents for the reduction processes for [M{-(R,R)-tetraphos](PF₆)₂ (M = Pd, Pt) were similar to the overall current for the two one-electron reduction processes of [Ni{(R,R)-tetraphos}](PF₆)₂ (or the one two-electron processes at low temperatures). On the basis of the peak current similarities, it was concluded that the reductions of [M{(R,R)-tetraphos}](PF₆)₂ (M = Pd, Pt) occur in one two-electron step over all temperatures measured, assuming that all three complexes have similar diffusion coefficients. Although the cyclic voltammograms of [M{(R,R)-tetraphos}]-(PF₆)₂ (M = Pd, Pt) show reverse peaks when the scan directions are switched, the wide ΔE_{pp} values observed on Pt and the very sharp peaks observed on GC indicate that the processes are more complicated than simple reversible electron transfer. It is possible that the reduction processes are associated with equilibria involving acetonitrile coordination to the palladium or platinum ions, as observed for the corresponding nickel complex.

Attempts to obtain cyclic voltammograms for [M₂{(R,R)-tetraphos}₂](OTf)₄ (M = Pd, Pt) were unsuccessful because the compounds could not be reduced within the potential window of the solvent/electrolyte (−3 V vs ferrocene).

Conclusion

The enantiomerically pure, linear, tetra(tertiary phosphine) (S,S)-tetraphos combines with nickel(II) chloride to give [NiCl{(R,R)-tetraphos}]Cl, which can be converted into [Ni{R,R)-tetraphos}](OTf)₂ by treatment with trimethylsilyl triflate; the latter complex shows reversible, sequential reductions to nickel(I) and nickel(0) in acetonitrile and dichloromethane at 20 °C. The complex [PdCl₂(SEt₂)₂] combines with (S,S)-tetraphos in acetonitrile to give a yellow solution from which colorless [Pd{(R,R)-tetraphos}](PF₆)₂ can be isolated by the addition of aqueous ammonium hexafluorophosphate. The mononuclear platinum(II) complex can be prepared similarly from [PtCl₂(COD)]. The CV of the mononuclear nickel(II) complex displays two one-electron reduction processes in acetonitrile at room temperature, whereas the corresponding palladium and platinum complexes each show one two-electron response of complex shape. When the reactions of (S,S)-tetraphos with [PdCl₂-(SEt₂)₂] or [PtCl₂(COD)] are carried out in dichloromethane and the intermediates are treated with trimethylsilyl triflate, the yellow solutions are decolorized immediately, and the complexes [M₂{R,R)-tetraphos}₂](OTf)₄ (M = Pd, Pt) can be isolated. The addition of a few drops of aqueous potassium chloride or sodium iodide to acetone-d_6 solutions of the dinuclear metal complexes brings about the immediate establishment of equilibrium mixtures containing the corresponding mononuclear metal complexes. The tetrahedral complex [Ni{(R,R)-tetraphos}] can be prepared from [Ni-

(COD)$_2$] and (*S,S*)-tetraphos in benzene, but it slowly rearranges into the more stable double-stranded helicate [Ni$_2$-{*R,R*)-tetraphos}$_2$] in solution, with which it is in equilibrium. The complexes [M$_2${(*R,R*)-tetraphos}$_2$] (M = Pd, Pt) can be prepared in high yields by the addition of (*S,S*)-tetraphos to solutions of [M(PPh$_3$)$_4$] in toluene (M = Pd) or benzene (M = Pt).

Experimental Section

Reactions involving the air-sensitive zerovalent metal complexes were performed under a positive pressure of nitrogen with the use of standard Schlenk techniques. Solvents were dried following the usual procedures and distilled under nitrogen before use. ^{31}P{^{1}H} NMR spectra were recorded in the solvents specified at 25 °C on Varian Inova 300 and 500 spectrometers operating at 121.42 and 202.42 MHz, respectively. The chemical shifts (δ) are reported in parts per million relative to external 85% aqueous H$_3$PO$_4$. Optical rotations were measured on the specified solutions in a 1 dm cell at 18 °C with a Perkin-Elmer Model 241 polarimeter. Specific rotations were estimated to be within ±0.5 deg cm^2 g^{-1}. ES MS were recorded on a Bruker Apex II 4.7T FTIR spectrometer with an Apollo ESI source. Elemental analyses were performed by staff within the Research School of Chemistry.

Enantiopure (*S,S*)-tetraphos[2] and the complexes [PdCl$_2$(SEt$_2$)$_2$],[28] [Pd(PPh$_3$)$_4$],[29] [PtCl$_2$COD],[30] and [Pt(PPh$_3$)$_4$][31] were prepared by literature methods. [Ni(COD)$_2$] was purchased from the Aldrich Chemical Co., Inc., and stored under argon in a Schlenk tube.

[*SP*-4-(4*R*$_P$,7*R*$_P$)]-(+)$_{546}$-(1,1,4,7,10,10-Hexaphenyl-1,4,7,10-tetraphosphadecane)nickel(II) Trifluoromethanesulfonate, [Ni-{(*R,R*)-tetraphos}](OTf)$_2$. A solution of [Ni(H$_2$O)$_6$]Cl$_2$ (0.048 g, 0.20 mmol) in water (5 mL) was added to a solution of (*S,S*)-tetraphos (0.13 g, 0.30 mmol) in dichloromethane (5 mL). The dropwise addition of ethanol (20 mL) to the vigorously stirred mixture afforded a deep red-brown precipitate of [NiCl((*R,R*)-tetraphos]Cl (0.15 g, 0.19 mmol). The solid was dissolved in dichloromethane (10 mL), and the deep red solution was cooled to 0 °C; TMSOTf (0.25 g, 1.11 mmol) was added to the solution, which changed color from deep red to yellow. After the mixture was stirred for 0.5 h, the solvent was removed from the reaction mixture under vacuum. The resulting solid was washed with diethyl ether to remove the TMSCl and excess TMSOTf. The solid was then dissolved in acetonitrile; dilution of the solution with diethyl ether afforded deep red crystals of the acetonitrile adduct, which, when filtered off, lost acetonitrile in vacuo to give the parent product as a bright yellow solid. Yield: 0.17 g (90%). mp: 231–234 °C. [α]$_{546}^{18}$: +16.1 (*c* 1, acetone). Anal. Calcd for C$_{44}$H$_{42}$F$_6$NiO$_6$P$_4$S$_2$: C, 51.43; H, 4.12. Found: C, 51.19; H, 4.35. ^{31}P{^{1}H} NMR (acetone-d_6): δ 45.4 (m, 2 P, $^2J_{PP(trans)}$ = 151 Hz, PPh$_2$), 110.3 (m, 2 P, $^2J_{PP(trans)}$ = 151 Hz, PPh). ES MS: *m/z* 1069.3 [M + 2OTf + CH$_3$CN + H]$^+$, 729.3 [M]$^+$, 366.3 [M + H]$^{2+}$. The crystallographic determination was carried out on a deep red crystal of the complex that had not been exposed to evacuation.

[*T*-4-[*M*$_{Ni}$,(4*R*$_P$,7*R*$_P$)]]-(−)-(1,1,4,7,10,10-Hexaphenyl-1,4,7,10-tetraphosphadecane)nickel(0), (*M*$_{Ni}$)-[Ni{(*R,R*)-tetraphos}]. A mixture of [Ni(COD)$_2$] (0.086 g, 0.30 mmol) and (*S,S*)-tetraphos (0.20 g, 0.30 mmol) was dissolved in benzene (5 mL) under argon. After 1 h, the solvent was removed from the bright yellow solution

under vacuum to leave an orange oil. The oil was dissolved in diethyl ether (7 mL); the pure product separated from the solution as a bright orange solid. Yield: 0.18 g (82%). mp: 98–101 °C. [α]$_D^{18}$: −147.9 (*c* 1, benzene). Anal. Calcd for C$_{42}$H$_{42}$NiP$_4$: C, 69.16; H, 5.80. Found: C, 69.55; H, 5.56. ^{31}P{^{1}H} NMR (C$_6$D$_6$): δ 49.5 (overlapping doublets, 2 P, $^2J_{PP}$ = 51.8 and 54.9 Hz, PPh$_2$), 69.1 (overlapping doublets, 2 P, $^2J_{PP}$ = 54.9 and 51.8 Hz, PPh). Orange plates of the monomeric complex and yellow plates of (*M*$_{Ni}$,*M*$_{Ni}$)-[Ni$_2${(*R,R*)-tetraphos}$_2$] crystallized above a diethyl ether solution of the monomeric complex, both of which were shown by X-ray crystallography to contain 0.5 diethyl ether molecule of crystallization.

[*SP*-4-(4*R*$_P$,7*R*$_P$)]-(+)-(1,1,4,7,10,10-Hexaphenyl-1,4,7,10-tetraphosphadecane)palladium(II) Hexafluorophosphate, [Pd-{(*R,R*)-tetraphos}](PF$_6$)$_2$. A mixture of (*S,S*)-tetraphos (0.10 g, 0.15 mmol) and [PdCl$_2$(SEt$_2$)$_2$] (0.053 g, 0.15 mmol) was dissolved in acetonitrile (5 mL). The yellow solution was stirred for 10 min before the addition of ammonium hexafluorophosphate (0.50 g, 3.07 mmol) in water (3 mL), which caused a color change in the solution to pale orange. The solvents were removed under vacuum, and water (10 mL) was added to dissolve the ammonium salts. The solid was filtered off and washed with water and diethyl ether, and the pale orange solid that remained was recrystallized from acetonitrile (4 mL) by the addition of diethyl ether (8 mL). The pure product crystallized from this solution as a colorless solid. Yield: 0.14 g (88%). mp: 174 °C (dec). [α]$_D^{18}$: +61.2 (*c* 1.0, acetone). Anal. Calcd for C$_{42}$H$_{42}$F$_{12}$P$_6$Pd: C, 47.28; H, 3.97. Found: C, 47.12; H, 4.02. ^{31}P{^{1}H} NMR (acetone-d_6): δ 42.2 (m, 2 P, $^2J_{PP(trans)}$ = 266 Hz, PPh$_2$), 108.9 (m, 2 P, $^2J_{PP(trans)}$ = 268 Hz, PPh), −143.1 (sept, 2P, $^1J_{PF}$ = 711.1 Hz, PF$_6$). ES MS: *m/z* 923.1 [M + PF$_6$ + H]$^+$, 777.2 [M]$^+$, 777.2 [M]$^+$, 389.2 [M]$^{2+}$.

[*SP*-4-(4*R*$_P$,7*R*$_P$)]-*M*$_H$-(−)-Bis(1,1,4,7,10,10-hexaphenyl-1,4,7,-10-tetraphosphadecane)dipalladium(II) Trifluoromethanesulfonate-2-Hydrate, [Pd$_2${(*R,R*)-tetraphos}$_2$](OTf)$_4$·2H$_2$O. A solution of (*S,S*)-tetraphos (0.10 g, 0.15 mmol) in dichloromethane (6 mL) was treated with a solution of [PdCl$_2$(SEt$_2$)$_2$] (0.053 g, 0.15 mmol) in dichloromethane (5 mL). After the mixture was stirred for 5 min, TMSOTf (0.067 g, 0.30 mmol) was added to the yellow solution, which was immediately decolorized. The reaction mixture was evaporated to dryness, and the colorless residue was recrystallized by dissolution in wet acetonitrile (8 mL) and slow addition of diethyl ether (12 mL). The pure complex was thus isolated as a colorless solid. Yield: 0.14 g (87%). mp: 312–315 °C. [α]$_D^{18}$: −311.7 (*c* 1, acetone). Anal. Calcd for C$_{88}$H$_{84}$F$_{12}$O$_{12}$P$_8$Pd$_2$S$_4$·2H$_2$O: C, 48.34; H, 4.06. Found: C, 48.26; H, 4.14. ^{31}P{^{1}H} NMR (acetone-d_6): δ 51.6 (br s, 4 P, PPh), 56.0 (br s, 4 P, PPh$_2$).

[*T*-4-[(*M*$_{Pd}$,*M*$_{Pd}$)-(4*R*$_P$,7*R*$_P$)]]-(+)-Bis(1,1,4,7,10,10-hexaphenyl-1,4,7,10-tetraphosphadecane)dipalladium(0), (*M*$_{Pd}$,*M*$_{Pd}$)-[Pd$_2$-{(*R,R*)-tetraphos}$_2$]. A solution of (*S,S*)-tetraphos (0.23 g, 0.35 mmol) and [Pd(PPh$_3$)$_4$] (0.4 g, 0.35 mmol) in toluene (5 mL) was stirred for 0.5 h. The yellow solution was then filtered through Celite to remove a trace of palladium. The solvent was removed from the solution under vacuum, and the resulting oil was dissolved in diethyl ether (8 mL). Bright yellow needles of the product separated overnight, which were collected, washed with diethyl ether, and dried under vacuum. Yield: 0.23 g (85%). mp: 125–128 °C (dec). [α]$_D^{18}$: +40.2 (*c* 1, benzene). Anal. Calcd for C$_{84}$H$_{84}$P$_8$Pd$_2$: C, 64.92; H, 5.45. Found: C, 64.56; H, 5.41. ^{31}P{^{1}H} NMR (C$_6$D$_6$): δ 33.7 (s). A small quantity of the complex was recrystallized from hot benzene, whereupon a yellow plate of the *2-benzene solvate* was isolated for the X-ray crystal structure determination.

(28) Clark, R. J. H.; Natile, G.; Belluco, U.; Cattalini, L.; Filippin, C. *J. Chem. Soc. A* **1970**, 659–663.
(29) Coulson, D. R. *Inorg. Synth.* **1990**, *28*, 107–109.
(30) Drew, D.; Doyle, J. R. *Inorg. Synth.* **1990**, *28*, 346–347.
(31) Ugo, R.; Cariati, F.; La Monica, G. *Inorg. Synth.* **1990**, *28*, 123–126.

[*SP*-4-(4*R*ₚ,7*R*ₚ)]-(−)-(1,1,4,7,10,10-Hexaphenyl-1,4,7,10-tet-raphosphadecane)platinum(II) Hexafluorophosphate, [Pt{(*R*,*R*)-tetraphos}](PF₆)₂. A solution of (*S*,*S*)-tetraphos (0.10 g, 0.15 mmol) and [PtCl₂(COD)] (0.055 g, 0.15 mmol) in acetonitrile (7 mL) was stirred for 10 min, and then a solution of ammonium hexafluoro-phosphate (0.50 g, 3.07 mmol) in water (3 mL) was added. After the mixture was stirred for a further 10 min, the solvents were removed from the solution by evacuation, and the pale yellow residue was stirred with water (10 mL) to dissolve the ammonium salts. The solid that remained was filtered off, washed with water and diethyl ether, and recrystallized from acetonitrile (5 mL) by the addition of diethyl ether (10 mL); the pure product crystallized from the solution as colorless microcrystals. Yield: 0.16 g (93%). mp: 270−272 °C. $[\alpha]_D^{18}$: −35.0 (*c* 1, acetone). Anal. Calcd for $C_{42}H_{42}F_{12}P_6Pt$: C, 43.65; H, 3.66. Found: C, 43.67; H, 3.92. $^{31}P\{^1H\}$ NMR (acetone-d_6): δ 42.0 (m + dm, 2 P, $^2J_{PP(trans)}$ = 272 Hz, $^1J_{PtP}$ = 2413 Hz, PPh₂), 95.7 (m + dm, 2 P, $^2J_{PP(trans)}$ = 283 Hz, $^1J_{PtP}$ = 2133 Hz, PPh), −142.8 (sept, 2 P, $^1J_{PF}$ = 708 Hz, PF₆). ES MS: m/z 1178.1 [M + 2PF₆ + Na]⁺, 1013.3 [M + PF₆]⁺, 866.2 [M + H]⁺, 432.8 [M]²⁺.

[*SP*-4-(4*R*ₚ,7*R*ₚ)]-(−)-Bis(1,1,4,7,10,10-hexaphenyl-1,4,7,10-tetraphosphadecane)diplatinum(II) trifluoromethanesulfonate−4.5-Hydrate, [Pt₂{(*R*,*R*)-tetraphos}₂](OTf)₄·4.5H₂O). This compound was prepared and isolated as previously described.[9] $^{31}P\{^1H\}$ NMR (300 MHz; acetone-d_6): δ 42.2 (br m, 4 P, $^1J_{PtP}$ = 2236 Hz, PPh), 47.8 (br m, 4 P, $^1J_{PtP}$ = 2405 Hz, PPh₂). ES MS: m/z 1165.2 [M + 2OTf + 2H]²⁺, 866.5 [M + H]²⁺.

[*T*-4-(4*R*ₚ,7*R*ₚ)]]-(−)-Bis(1,1,4,7,10,10-hexaphenyl-1,4,7,10-tet-raphosphadecane)diplatinum(0), [Pt₂{(*R*,*R*)-tetraphos}₂]. A mixture of (*S*,*S*)-tetraphos (0.20 g, 0.30 mmol) and [Pt(PPh₃)₄] (0.30 g, 0.24 mmol) was dissolved in benzene (5 mL). After the mixture was stirred for 0.5 h, the solvent was removed under vacuum from the yellow solution. The yellow oil that remained was dissolved in diethyl ether (8 mL), whereupon a yellow solid separated immediately. The solid was collected, washed thoroughly with diethyl ether, and dried under vacuum to give the pure complex as a deep yellow powder. Yield: 0.11 g (53%). mp: 162−166 °C. $[\alpha]_D^{18}$:

−117.6 (*c* 1, benzene). Anal. Calcd for $C_{84}H_{84}P_8Pt_2$: C, 58.27; H, 4.89. Found: C, 58.14; H, 4.76. $^{31}P\{^1H\}$ NMR (C_6D_6): δ 29.2 (m, 4 P, PPh₂), 38.4 (m, 4 P, PPh).

Crystal Structures. Crystal data and experimental parameters for the complexes are given in Table 1. The software used for the structural solutions of the four complexes was SIR92.[35]

Spectroscopy and Electrochemistry. In situ UV−vis spectra were obtained with use of a Varian Cary 5E spectrophotometer in an optically transparent thin layer electrochemical (OTTLE) cell (path length = 0.05 cm) at −20 °C using a platinum mesh working electrode. The typical exhaustive electrolysis period for the one-electron reduction of 1 mM analyte in dichloromethane containing 0.5 M [(*n*-Bu)₄N]PF₆ was 1 h. Voltammetric experiments were conducted with a computer-controlled Eco Chemie mAutolab III potentiostat. The electrochemical cell was jacketed in a glass sleeve and cooled from 20 to −40 °C using a Lamda RL6 variable temperature methanol-circulating bath. Cyclic voltammetry experiments were conducted with 1 mm diameter planar glassy carbon (GC) or platinum (Pt) electrodes.

Supporting Information Available: Additional crystallographic data in CIF format and electrochemical data. This material is available free of charge via the Internet at http://pubs.acs.org.

IC700912Q

(32) Watkin, D. J.; Prout, C. K.; Carruthers, J. R.; Betteridge, P. W. *CRYSTALS*, issue 10; Chemical Crystallography Laboratory: Oxford, U.K., 1996.

(33) Mackay, S.; Gilmore, C. J.; Edwards, C.; Stewart, N.; Shankland, K. *maXus Computer Program for the Solution and Refinement of Crystal Structures*; Nonius: Delft, The Netherlands; MacScience: Japan; University of Glasgow: Glasgow, U.K., 1999.

(34) Rae, A. D. *RAELS2000*; Australian National University: Canberra, Australia, 2000.

(35) Altomare, A.; Cascarano, G.; Giacovazzo, C.; Guagliardi, A.; Burla, M. C.; Polidari, G.; Camalli, M. *J. Appl. Crystallogr.* **1994**, *27*, 435.